Original Article

An optimized non-local means filter using automated clustering based preclassification through gap statistics for speckle reduction in breast ultrasound images

K.M. Prabusankarlal [a,*], R. Manavalan [b], R. Sivaranjani [c]

[a] Department of Electronics & Communication, K.S. Rangasamy College of Arts & Science, Tiruchengode 637215, India
[b] Department of Computer Science & Applications, Arignar Anna Government Arts College, Villupuram 605602, India
[c] Department of Mathematics, K.S.R. College of Arts & Science for Women, Tiruchengode 637215, India

ARTICLE INFO

ABSTRACT

Speckle noise is a characteristic artifact in breast ultrasound images, which hinders substantive information essential for clinical diagnosis. In this article, we have investigated the use of Non-local means (NLM) filter, which is robust against severe noise, to remove speckle noise in breast ultrasound images. Medical diagnosis systems cannot employ traditional NLM filters, which exhibit the slowest performance due to their computational burden during the weighted averaging process. We have integrated a novel automated clustering based preclassification scheme using spatial regularized fuzzy c means (FCM) to alleviate the process. The appropriate number of clusters for each image is calculated automatically through Gap statistics. Moreover, the rotationally invariant moment distance measure increases the chance of getting more similar regions for NLM process. The algorithm is evaluated on a breast ultrasound database, which consists of 54 images including 28 benign and 26 malignant. Two statistical measures, Pratt's figure of merit (PFM) and equivalent number of looks (ENL), are used to evaluate the noise suppression performance as well as the capability of preserving the fine details. The results of the proposed method are compared with the other three state of the art methods quantitatively. The proposed method demonstrated excellent despeckling performance with PFM of 0.91 and ENL of 7.415. The robustness against speckle noise and the acceptable processing time make the method more appropriate for computer aided diagnosis systems.

1. Introduction

Worldwide, breast cancer is the most frequently diagnosed cancer in women and accounts for 14% in overall cancer deaths [1]. Early detection and diagnosis of breast cancer increase the survivability of patients and reduce mortality [2,3]. Ultrasound imaging is an effective, convenient, inexpensive and radiation-free imaging tool for breast tumor diagnosis [4]. Ultrasound has higher sensitivity for detecting lesions in dense breasts, commonly found among young women [5]. Reduced rate of false-positive results in ultrasound brings down the number of unnecessary biopsies, when compared to mammography [6]. Since the tumor contour is the most important information for diagnostic decision, the physician could observe more clearly the difference in shapes and sizes of malignant and benign breast lesions using ultrasound [7].

Many ultrasound computer aided detection and diagnosis (CAD) systems have been developed to provide computerized estimation of the probability of malignancy [8]. The traditional B-mode grayscale ultrasound remains the standard in the clinic due to physicians' familiarity with it [9]. However, the most important deficiency of ultrasound is the poor quality of the image, when it is corrupted by speckle noise during the acquisition process. The existence of the speckle ruins the image quality and impacts the diagnosis accuracy [10,11]. The objective of image denoising task is to remove the speckle noise while retaining the signal features as much as possible in order to increase the diagnostic accuracy. An accurate model of speckle noise formation is necessary for the development of a despeckling algorithm. Although many statistical

* Corresponding author.
 E-mail address: kmsankar@gmail.com (K.M. Prabusankarlal).

models were developed to describe speckle noise, there is no universally accepted model available yet. However a general model [12] for speckle noise is given as $g(n,m) \simeq f(n,m)u(n,m)$, where $g(n,m)$ is the observed image, $f(n,m)$ is the original image and $u(n,m)$ multiplicative component of speckle noise.

Typically, speckle reduction is accomplished by applying various filters. However, these filters also remove finer edge details, which are essential for producing an accurate contour of the tumor for diagnosis [13]. Directional average filter [14], and partial differential equation (PDE) based filters [15–19] are able to preserve important features such as edges, corners and point targets, while removing speckle noise in ultrasound images. The anisotropic diffusion (AD) filter [15] utilizes the local estimations of the image structures where the image smoothing is devised as a diffusive process and it is stopped at lesion boundaries to preserve the discontinuities. Filters such as speckle reducing AD (SRAD) [16], adaptive window AD (AWAD) [17], oriented SRAD [18] and speckle suppressing AD (SSAD) [19] were also utilized for despeckling ultrasound images. Although the PDE based methods exhibited improved speckle reduction and edge preservation, they lose meaningful details during iterations by producing blurred low con-

trast edges and speckle is often retained in the high intensity regions. Moreover, in all these methods, the restored value of a pixel only depends on its spatial neighborhood pixels of the same image context, known as locally adaptive recovery paradigm [20].

Buades et al. [21] proposed non-local means (NLM) approach, which exploits specific characteristics of natural or texture images such as repetitive patterns. NLM filter is based on the category of directional average filters [14] and it replaces each pixel with a weighted average of other pixels with similar neighborhoods. The NLM filer produced the promising results on severely noise affected images [21–27] and ultrasound images [28–31]. The drawback of the NLM algorithm is that it consumes more processing time during the calculation of weights. Many methods were proposed to speed up the processing by eliminating dissimilar patches before the weight calculation. Techniques such as preselection of contributing neighborhoods based on mean and gradient values [24], use of local mean and variance to eliminate dissimilar pixels [23], use of fast Fourier transform (FFT) [25] and utilization of several critical pixels in the center instead of all neighborhood pixels [26] were used during the calculation of weights. Grewenig et al. [27] used two similarity measures: moment invariants and rotationally invariant block matching (RIBM). The method identified similar patches present in several rotated or mirrored instances to obtain more suitable regions. This method improved the despeckling performance of NLM considerably, but not the processing speed. Zhan et al. [31] introduced a weight refining NLM method, where weight calculation is performed in lower dimensional subspace using PCA instead of the original noisy image space to reduce computational cost. Although the preselection process improves the preservation of detail rich regions, the flat regions are slightly degraded [28]. In fact the flat regions contain a large number of similar pixels, which tends to improve denoising performance. Yan et al. [32] presented the concept of clustering based preclassification to increase the computational speed without

Table 1
Details of the parameters used for the experiments.

Methods	Details of parameters
Image database	Breast ultrasound images (B mode) Dimension of images 256×256. Format: TIFF
Moment invariants used	Hu's seventh moment invariants φ_7
Number of clusters c for FCM	Automatically set by gap statistics, $m = 2$, $\alpha = 0.8$, and $N_R = 9$ 3×3 window)
Block (patch) and search window size	5×5 and 21×21; common for all images
Filtering parameter h	Global parameter $h = 15$
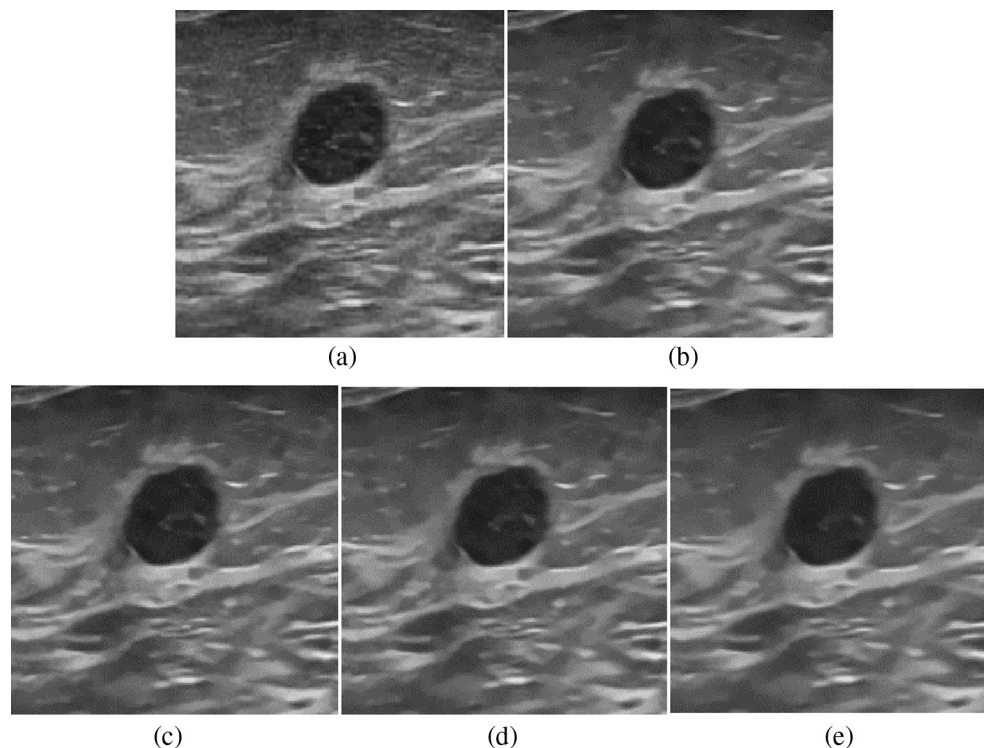
Fig. 1. A Benign cyst has smooth and regular contour edges. A specific benign image (Image_ID: U5) processed by different methods for visual comparison: (h = 15, clusters = 1188) (a) original (b) method [27] (c) method [33] (d) method [39] and (e) proposed method.

elimination of pixels. The computational intensity is alleviated considerably by performing the weighted averaging within each cluster. The filter produced superior quantitative results when the appropriate number of clusters with sufficient number of pixel candidates is chosen manually.

In this article, we have proposed a novel framework for NLM filter to remove speckle noise in breast ultrasound images. We have integrated an automated clustering based preclassification scheme into the NLM model to increase the computational speed as well as the noise reduction performance. During preclassification process, feature vectors are calculated for the image using moment invariants and are clustered by spatial regularized FCM algorithm. Meanwhile, the gap statistics automatically calculate the appropriate number of clusters for each image. The weighted averaging process is performed using RIBM within each cluster and it identifies more similar regions in an image. Thus, the NLM has been facilitated with more suitable regions without eliminating any pixel candidates to yield superior denoising performance with reduced processing time.

2. Methods

2.1. The image database

The image database consists of 54 B-mode breast ultrasound images including 28 benign and 26 malignant cases. These images were acquired through high end ultrasound system (Prosound F75, Hitachi medical systems Europe, Switzerland) from different patients over different periods with the consent of the patients [33]. It complies with the HONcode (health on the net foundation) standard for trustworthy health information. The study protocols are approved by institution's ethics committee of Gelderse Vallei Hospital, Ede, the Netherlands.

2.2. The NLM algorithm

The NLM algorithm makes use of the self similarity of patches in an image [21]. In an image, the restored intensity $NL(v)(i)$ of a pixel i is a weighted average of all intensity values within the neighborhood I. The traditional NLM [21] is given by $NL(v)(i) = \sum_{j \in I} \omega(i,j) v(j)$, where v is the intensity, $v(j)$ is the intensity at pixel j, and $\omega(i,j)$ is the assigned weight. The weights $\omega(i,j) = \frac{1}{Z(i)} e^{-\frac{\|vN_i - vN_j\|_2^2}{h^2}}$ depend on the similarity between the intensities of the local neighborhood patches (blocks) centered on pixel i and j. Where N_i is a patch of fixed size and centered at the pixel i. The similarity term $\| \cdot \|_2^2$ is computed between weighted Euclidean distance of vN_j (neighborhood of j) and vN_i (neighborhood of i). $Z(i)$ is the normalization constant ensuring that $\sum_{j \in I} \omega_R(i,j) = 1$. The h is the filtering parameter which controls the smoothing. The improved NLM [32] is given as $NL(v)(i) = \sum_{j \in L} \omega_R(i,j) v(j)$, where the modified weight $\omega_R(i,j)$ defined as $\omega_R(i,j) = \frac{1}{Z_R(i)} e^{-\frac{d_R(i,j)}{h^2}}$. The $\omega_R(i,j)$ depends on distance measure $d_R(i,j)$ which is defined in Section 2.5 and the L is the number of elements in a cluster. The computational time can be reduced by performing calculation of weights within each cluster instead for the entire image.

2.3. Pre-classification using spatial regularized FCM clustering

The Hu's moment invariant [27] is used as image descriptor. For an $N \times M$ image with an $N \times M$ patch centered at location i, where $(i = 1,2,3,\ldots,N \times M)$, the moment invariants of the patch are represented by a vector of (1×7). Totally, $(N \times N)$ vectors for the entire image are constructed. The clustering based preclassification

is performed for defining a set of candidates that contains different patches from all over the image, which serve as lookup table (LUT) for block matching process. The spatial regularized FCM is used as clustering algorithm. The objective function is defined as follows:

$$J_m = \sum_{i=1}^{c} \sum_{k=1}^{N} \mu_{ik}^m \|x_k - v_m\|^2 + \frac{\alpha}{N_R} \sum_{i=1}^{c} \sum_{k=1}^{N} \mu_{ik}^m \left(\sum_{x_r \in N_k} \|x_r - v_m\|^2 \right) \quad (1)$$

where x_r is the neighbor of x_k; N_k is a set of neighbors within a window around x_k and N_R is the cardinality of N_k. The parameter α controls the neighborhoods and its relative importance is inversely proportional to the amount of noise present in the image.

2.4. Calculating number of clusters using gap statistics

Tibshirani et al. [35] discovered that the "within cluster dispersion", an error measure decreases when the number of clusters 'k' increases. However, when a specific value of 'k' is reached, the error measure becomes flat. The value of 'k' at such an 'elbow', indicates the appropriate number of clusters and it can be assigned to any clustering algorithm automatically.

At first the input image data x_{ij} $(i = 1,2\ldots,n$ and $j = 1,2, \ldots,m)$ are clustered by changing the total number of clusters from $k = 1,2,3,\ldots,k_n$, where the m features are measured in n independent observations. The distance between two observations i and i'. $d_{ii'}$ where the same can be calculated through squared Euclidean distance $\sum_j (x_{ij} - x_{i'j})^2$. The C_r denotes the indices of n cluster r, if the clustered data are $C_1, C_2, \ldots, C_k$ and $nr = |C_r|$. The within cluster dispersion W_k, an error measure [36] is given as follows:

$$W_k = \sum_{r=1}^{k} \frac{1}{2n_r} D_r \quad (2)$$

where D_r, the sum of pair wise distances in cluster r is calculated by $D_r = \sum_{i,i' \in C_r} d_{ii'}$. We compare the graph [35] of $\log(W_k)$ to its expectation under an appropriate null reference distribution of data. The optimum number of clusters is estimated by finding the value of k for which $\log(W_k)$ falls below this reference curve. The $G_n(k)$ is estimated as follows:

$$G_n(k) = E_n(\log(W_k)) - \log(W_k) \quad (3)$$

where the E_n denotes the expectation under a sample size of n from the reference distribution. Generate B reference datasets as prescribed in [35], and cluster each one $k = 1,2,\ldots,K$ and find within cluster dispersion measure W_{kb} for $b = 1,2,\ldots,B$. Compute the gap $G_n(k)$ using Eq. (3).

$$G_n(k) = \frac{1}{B} \sum_b (\log(W_{kb}) - \log(W_k)) \quad (4)$$

Compute the standard deviation of B as $SD_k = \left[\frac{1}{B} \sum_b (\log(W_{kb}) - \bar{h}) \right]^{\frac{1}{2}}$ where $\bar{h} = \frac{1}{B} \sum_b (\log(W_{kb}))$ and $S_k = SD_k \sqrt{1 + 1/B}$. Finally choose the smallest size of k as $\hat{k}$.

$$\hat{k} = smallest\ k\ such\ that\ G_n(k) = G_n(k+1) - S_{k+1} \quad (5)$$

This k value is assigned to the spatial regularized FCM algorithm as $k = c$.

2.5. RIBM based nonlocal filtering

In NLM algorithm, lack of repetitive patterns in an image leads to insufficient candidates for weighted averaging. Also, the use of moment invariants during preclassification might have possibly left rotationally unaligned candidates at neighborhood. The RIBM can solve these problems by finding similar regions
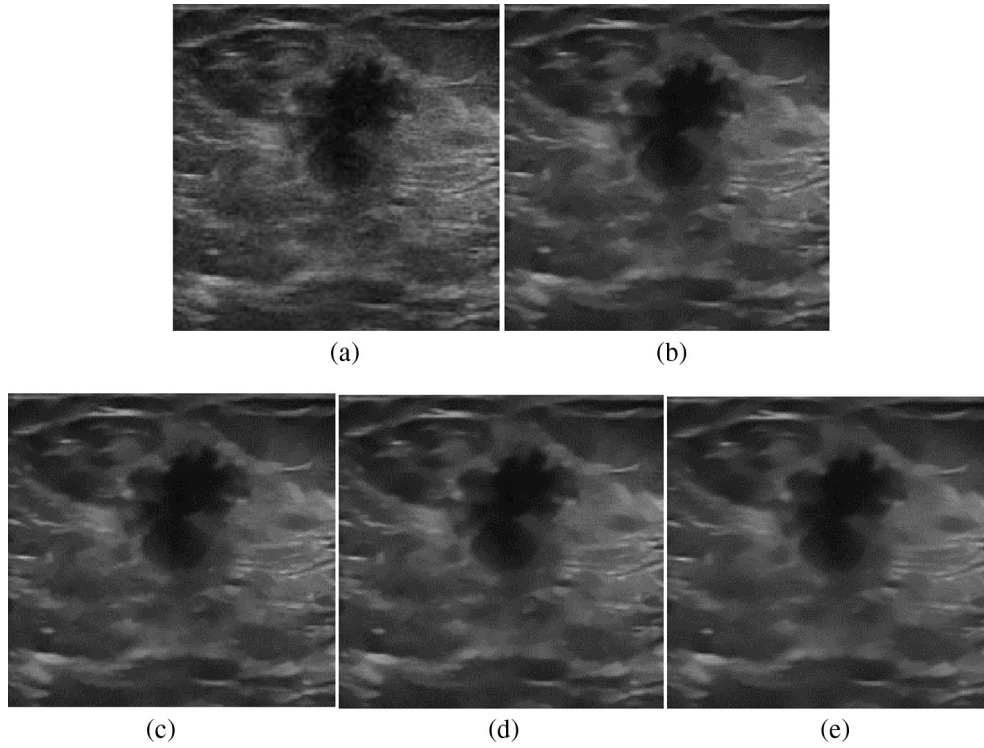
Fig. 2. A Malignant tumor image characterized by irregular shapes with rough contour edges. A specific malignant image (Image_ID: U45), processed by different methods: (h = 15, clusters = 1120) (a) original (b) method [27] (c) method [33] (d) method [33] and (e) proposed method.

Table 2
The PFM and ENL values of the methods under comparison with common parameter settings. The values are the mean values of entire database (both benign and malignant images). The p values are calculated through ANOVA test.

Parameters	Traditional NLM	NLM with RIBM	Improved NLM	Proposed method	p value	Statistical significance
PFM	0.7	0.759	0.819	0.91	<0.05	Yes
ENL	5.566	5.829	6.031	7.415	<0.05	Yes
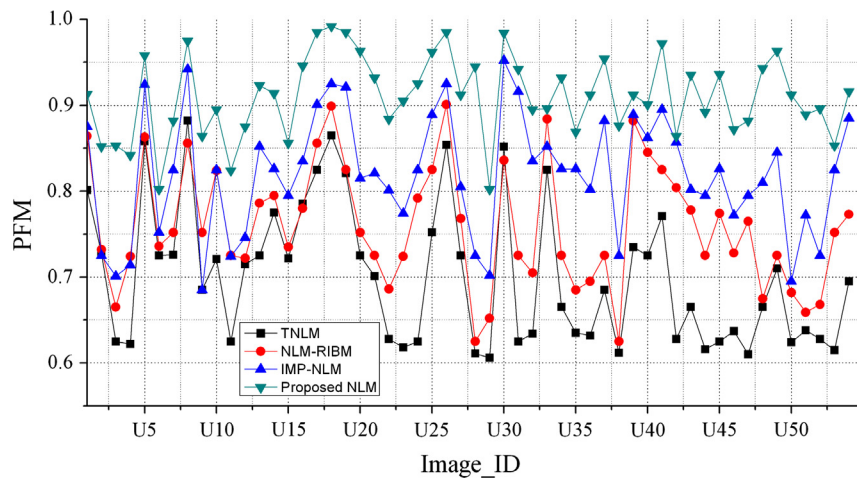
Fig. 3. Pratt's figure of merit (PFM) is used as a metric to evaluate the preservation of edges.

in an image [36]. The RIBM estimates the angle of rotation between two blocks by its centroid and using this value, it finds the position of the corresponding pixel in another block by rotating its vector. The new similarity measure in discrete form is given as [32]:

$$d_R(N_i, N_j) = \sum_{c_i \in N_i} (f_{N_i}(c_i) - I(f_{N_j}, c_j)^2 dc_i \qquad (6)$$

where I denotes bilinear interpolation function. For each point of c_i in patch N_i, after rotation and interpolation, its corresponding point c_j in patch N_j is obtained.

2.6. Selection of parameters for experiment

The parameters used for our experiments are listed in Table 1. Hu's seventh moment invariant φ_7 is used as feature descriptor in preclassification. The appropriate number of clusters for preclassification is determined by gap statistics. The block size of 5×5 is chosen for RIBM and the size of the search window is set at 21×21 [21,37,38]. The filter parameter h is an important parameter in NLM filter. The optimal value of h depends on the amount of noise present in the image. Choosing a low value of h leads to noisy image and a high value of h blurs the fine details of image. In many methods [31] the value of h is chosen as $h = C\sigma$ where C is a constant and σ is the standard deviation of noise. As we confine our experiments with breast ultrasound images, the noise cannot be estimated and so we have chosen $h = 15$ as suggested in [36,27].

3. Results

The method is evaluated on breast ultrasound image database, using two statistical parameters namely Pratt's figure of merit (PFM) [16] and equivalent number of looks (ENL) [30]. We have compared the results of the proposed method with other three state of the art NLM based methods: traditional NLM (TNLM) [21], NLM with RIBM [27] and improved NLM [32]. In our experiments, the same set of NLM parameters (Table 1) are used for all these methods. In the Figs. 1 and 2, (a) is the original image from the database, (b) the processed image by the method [21], (c) by the method [27], (d) by the method [32] and (e) shows the processed image by our method. Table 2 shows numerical results produced by all the evaluated methods. The values shown are the mean values of entire images in the database. An ANOVA test is also performed to analyze significant improvements in the denoising performance of the proposed algorithm over other methods. As shown in Table 2, the proposed method produced PFM and ENL values of 0.91 and 7.415 respectively, which are significantly higher than the other three methods with all p values < 0.05. The values of PFM and ENL for each individual image are plotted in Figs. 3 and 4 for comparison. All algorithms have been run on Matlab 2009a (Mathworks Inc., USA), in an Intel Core i5 processor (Intel Corp., USA) based PC with 8 GB RAM.

4. Discussion

We have presented a NLM based method for removing speckle noise from breast ultrasound images by considering its robustness against heavy noise [21]. The traditional NLM is a simple and effective way to reduce noise, while keeping details of the images unaffected. A limitation of the filter is that it can identify patches as similar to a given patch with same structure and orientation but similar patches with similar structure but different orientations do not have influence in the average [39]. To rectify this issue, the orientation of patches is estimated and corrected before weighted averaging process using RIBM [27,36] to obtain more suitable regions.

The lower processing time is an important criterion for medical image denoising. So we have concentrated methods, which reduce computational time. Yan et al. [32] used clustering based preclassification [32] to achieve faster processing without the elimination of any pixels in weight calculation. The k-means algorithm is used for clustering, where the value of k (number of clusters) has been set manually though visual perception as well as through peak signal to noise ratio (PSNR) values. In k-means algorithm, the patches are divided into distinct clusters and each element of a patch belongs to exactly one cluster. This restricts the candidates to be present in more than one cluster. Such a restriction is not present in fuzzy clustering where the elements of a patch can spread over
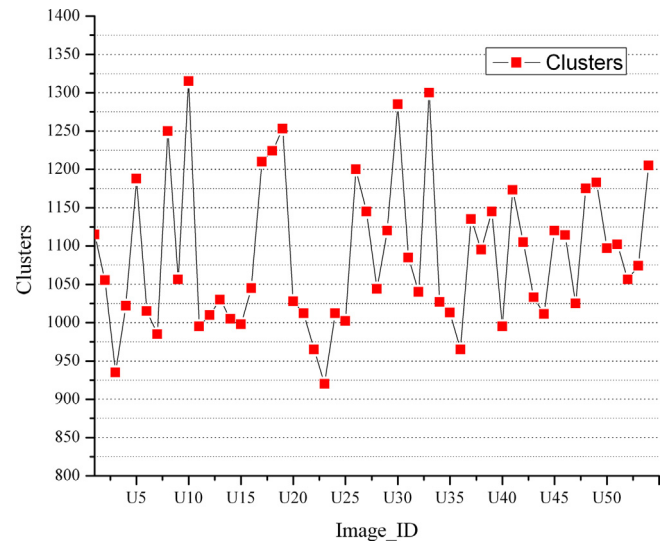
Fig. 5. The graph shows appropriate number of clusters automatically selected for each image through gap statistics. The number of clusters varied from 920 to 1315 for the 54 images in the database.
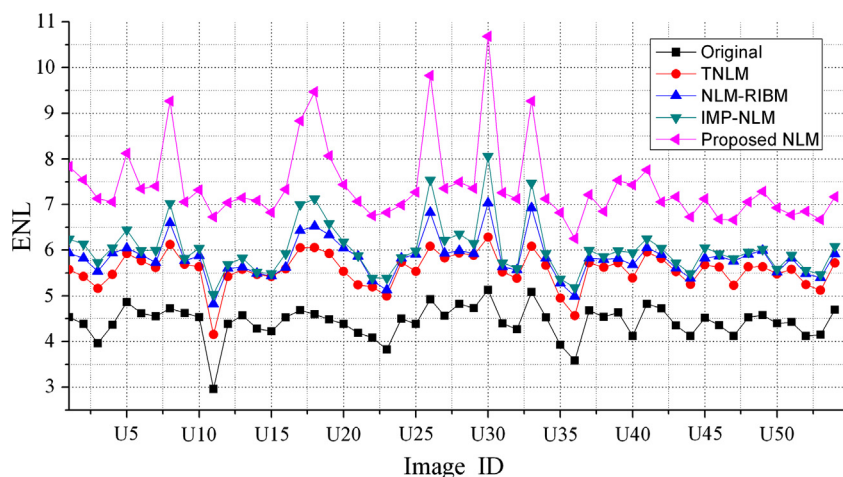
Fig. 4. Equivalent number of looks (ENL) is an inherent parameter for measuring noise level in an image. ENL is calculated from a small rectangular homogeneous region of the images.

more than one cluster with an association defined by a membership function. This property increases the probability of getting more suitable candidates from each cluster for weighted averaging. However, the FCM does not consider the spatial information in the image context [34], which makes it very sensitive to noise and other imaging artifacts. In spatial regularized FCM algorithm, the local spatial information is incorporated into the FCM [34], in which the neighborhood effect acts as a regularizer.

Moreover, in clustering based preclassification methods, the number of clusters impacts the denoising performance [32] and the estimation of optimum number of clusters is the major challenge. If the number of clusters is more, fewer candidates are present in each cluster and degrade the denoising performance. In contrary, if clusters are less, more number of candidates are present in each cluster and make the method sluggish. In our work, we have used gap statistics [35] to choose appropriate number of clusters which leads to optimum performance. The curve in Fig. 5 shows the appropriate values of k produced for each image of our database. It can be observed from the graph that the value of k is unique for each image, which varies from 920 to 1315.

The PFM is used as a metric to evaluate the preservation of edges. It uses the distance between all pairs of points to quantify the quality of edges. It is observed from the curves (Fig. 3) that our method produced PFM values comparatively higher for the most of the images in the database, which demonstrates better edge preservation. The range of PFM is between 0 and 1 and higher value is for ideal edge detection. Canny's method, which produces single response for each selected edges is used for edge detection [16] with standard deviation of the Gaussian kernel $\sigma = 0.1$. We achieved a higher PFM of 0.91, when compared to other methods: TNLM (0.7), NLM-RIBM (0.759) and improved NLM (0.819). The inherent parameter, ENL is an effective index for estimating the speckle noise level in images [30]. The value of ENL corresponds to smoother homogeneous region in the despeckled image. The comparison of ENL values is shown in Fig. 4. The ENL is calculated on a small rectangular homogeneous region in the original image and the value obtained is 4.43. The proposed method produced higher value of ENL (7.415), when compared to TNLM (5.566), NLM with RIBM (5.829) and improved NLM (6.031), manifests better despeckling ability over other methods. The TNLM [24] consumed 28 s, the method [27] consumed 31 s, the method [32] consumed 6.8 s and the proposed method consumed 7.2 s. The processing time of the proposed method (7.2 s) is slightly higher than the method [32] (6.8 s), because of the implementation of gap statistic in preclassification stage. The acceptable processing time and the ability of preserving image details while removing speckle noise make it suitable for computer aided diagnosis systems.

5. Conclusion

In this article, we have presented a novel NLM framework for removing speckle noise in breast ultrasound images. The proposed method has improved the NLM performance in two ways: an automated clustering based preclassification scheme through gap statistics and a new similarity measure using rotationally invariant moment distance measure. The results have shown that the presented method gives better quantitative results compared to other state-of-the-art NLM based methods. Thus, the robustness against noise and low processing time make the filter appropriate for ultrasound computer aided breast cancer diagnosis systems.

References

[1] A. Jemal, F. Bray, M.M. Center, J. Ferlay, E. Ward, D. Forman, Global cancer statistics, CA Cancer J. Clin. 61 (2011) 69–90.

[2] S. Khan, M. Hussain, H. Aboalsamh, G. Bebis, A comparison of different Gabor feature extraction approaches for mass classification in mammography, Multim. Tools Appl. (2015) 1–25.

[3] T. Jia-Wei, N. Chun-Ping, G. Yan-Hui, C. Heng-Da, T. Xiang-Long, Effect of a novel segmentation algorithm on radiologists' diagnosis of breast masses using ultrasound imaging, Ultrasound Med. Biol. 38 (1) (2012) 119–127.

[4] S. Zhou, J. Shi, J. Zhu, Y. Cai, R. Wang, Shearlet-based texture feature extraction for classification of breast tumor in ultrasound image, Biomed. Signal Process. Control 8 (6) (2013) 688–696.

[5] J.L. Jesneck, J.Y. LoY, J.A. Baker, Breast mass lesions: computer-aided diagnosis models with mammographic and sonographic descriptors, Radiology 244 (2007) 390–398.

[6] G. Pons, J. Martí, R. Martí, S. Ganau, J.C. Vilanova, J.A. Noble, Evaluating lesion segmentation on breast sonography as related to lesion type, J. Ultrasound Med. 32 (9) (2013) 1659–1670.

[7] Y.L. Huang, D.R. Chen, S.C. Chang, Three-dimensional region-based segmentation for breast tumors on sonography, J. Ultrasound Med. 32 (5) (2013) 835–846.

[8] K. Drukker, N.P. Gruszauskas, C.A. Sennett, M.L. Giger, Breast US computer-aided diagnosis workstation: performance with a large clinical diagnostic population, Radiology 248 (2) (2008) 392.

[9] A. Athanasiou, A. Tardivon, L. Ollivier, F. Thibault, C.E. Khoury, S. Neuenschwander, How to optimize breast ultrasound, Eur. J. Radiol. 69 (1) (2009) 6–13.

[10] I. Njeh, O.B Sassi, K Chtourou, A.B Hamida, Speckle noise reduction in breast ultrasound images: SMU (SRAD Median Unsharp) approach, in: Proceedings of the Eighth IEEE International Multi Conference on Systems, Signals and Devices, 2011, pp. 1–6.

[11] K.M. Prabusankarlal, P. Thirumoorthy, R. Manavalan, Computer aided breast cancer diagnosis techniques in ultrasound: a survey, J. Med. Imag. Health Inf. 4 (3) (2014) 331–349.

[12] O.V. Michailovich, A. Tannenbaum, Despeckling of medical ultrasound images, IEEE Trans. Ultrason. Ferroelectr. Freq. Control 53 (1) (2006) 64–78.

[13] H.D. Cheng, J. Shan, W. Ju, Y. Guo, L. Zhang, Automated breast cancer detection and classification using ultrasound images: a survey, Pattern Recogn. 43 (1) (2010) 299–317.

[14] Y. Guo, H.D. Cheng, J. Tian, Y. Zhang, A novel approach to speckle reduction in ultrasound imaging, Ultrasound Med. Biol. 35 (4) (2009) 628–640.

[15] P. Perona, J. Malik, Scale-space and edge detection using anisotropic diffusion, IEEE Trans. Pattern Anal. Mach. Intell. 12 (7) (1990) 629–639.

[16] Y. Yu, S.T. Acton, Speckle reducing anisotropic diffusion, IEEE Trans. Image Process. 11 (11) (2002) 1260–1270.

[17] G. Liu, X. Zeng, F. Tian, Z. Li, K. Chaibou, Speckle reduction by adaptive window anisotropic diffusion, Signal Process. 89 (11) (2009) 2233–2243.

[18] K. Krissian, C.F. Westin, R. Kikinis, K.G. Vosburgh, Oriented speckle reducing anisotropic diffusion, IEEE Trans. Image Process. 16 (5) (2007) 1412–1424.

[19] S. Ovireddy, E. Muthusamy, Speckle suppressing anisotropic diffusion filter for medical ultrasound images, Ultrason. Imag. 36 (2) (2014) 112–132.

[20] M. Elad, On the origin of the bilateral filter and ways to improve it, IEEE Trans. Image Process. 11 (10) (2002) 1141–1151.

[21] A. Buades, B. Coll, J.M. Morel, A review of image denoising algorithm, with a new one, Simulation 4 (2005) 490–530.

[22] A. Buades, B. Coll, J.M. Morel, Image denoising methods. A new nonlocal principle, SIAM Rev. 52 (1) (2010) 113–147.

[23] P. Coupé, P. Yger, S. Prima, P. Hellier, C. Kervrann, C. Barillot, An optimized blockwise nonlocal means denoising filter for 3-D magnetic resonance images, IEEE Trans. Med. Imaging 27 (4) (2008) 425–441.

[24] M. Mahmoudi, G. Sapiro, Fast image and video denoising via nonlocal means of similar neighborhoods, IEEE Signal Process. Lett. 12 (2005) 839–842.

[25] J. Wang, Y. Guo, Y. Ying, Y. Liu, Q. Peng, Fast non-local algorithm for image denoising, in: Proceedings of the IEEE International Conference on Image Processing, 2006, pp. 1429–1432.

[26] P. Chao, O.C. Au, D. Jingjing, Y. Wen, Z. Feng, A fast NL-means method in image denoising based on the similarity of spatially sampled pixels, in: Proceedings of the IEEE International Workshop on Multimedia Signal Processing, 2009, pp. 1–4.

[27] S. Grewenig, S. Zimmer, J. Weickert, Rotationally invariant similarity measures for nonlocal image denoising, J. Vis. Commun. Image R. 22 (2011) 117–130.

[28] P. Coupé, P. Hellier, C. Kervrann, C. Barillot, Nonlocal means-based speckle filtering for ultrasound images, IEEE Trans. Image Process. 18 (10) (2009) 2221–2229.

[29] Y. Guo, Y. Wang, T. Hou, Speckle filtering of ultrasonic images using a modified non local-based algorithm, Biomed. Signal Process. Control 6 (2) (2011) 129–138.

[30] Y. Gu, Z. Cui, C. Xiu, L. Wang, Ultrasound echocardiography despeckling with non-local means times series filter, Neurocomputing 124 (2013) 120–130.

[31] Y. Zhan, M. Ding, L. Wu, X. Zhang, Nonlocal means method using weight refining for despeckling of ultrasound images, Signal Process. 103 (2014) 201–213.

[32] R. Yan, L. Ling Shao, S.D. Cvetkovic, J. Klijn, Improved nonlocal means based on pre-classification and invariant block matching, IEEE J. Display Technol. 8 (4) (2012) 212–218.

[33] Ultrasoundcases <http://ultrasoundcases.info/category.aspx?cat=67> (accessed July 2014).

[34] K.M. Prabusankarlal, P. Thirumoorthy, R. Manavalan, Segmentation of breast lesions in ultrasound images through multiresolution analysis using undecimated discrete wavelet transform, Ultrason. Imag. 38 (6) (2016) 384–402.

[35] R. Tibshirani, G. Walther, T. Hastie, Estimating the number of clusters in a data set via the gap statistic, J. R. Statist. Soc.: Ser. B (Statist. Methodol.) 63 (2) (2001) 411–423.

[36] S. Zimmer, S. Didas, J. Weickert, A rotationally invariant block matching strategy improving image denoising with non-local means, in: Proceedings of the 2008 International Workshop on Local and Non-Local Approximation in Image Processing, 2008, pp. 135–142.

[37] J. Salmon, On two parameters for denoising with non-local means, Signal Process. Lett. IEEE 17 (3) (2010) 269–272.

[38] K.M. Prabusankarlal, P. Thirumoorthy, R. Manavalan, Assessment of combined textural and morphological features for diagnosis of breast masses in ultrasound, Human-Centric Comput. Inf. Sci. 5 (1) (2015) 1–17.

[39] J.V. Manjón, P. Coupé, A. Buades, D. Louis Collins, M. Robles, New methods for MRI denoising based on sparseness and self-similarity, Med. Image Anal. 16 (1) (2012) 18–27.